Mineralogical Magazine, April 2008, Vol. 72(2), pp. 563–568

Assessment of crystallographic influence on material properties of calcite brachiopods

A. PÉREZ-HUERTA[1], M. CUSACK[1,*] AND W. ZHU[2]

[1] Department of Geographical and Earth Sciences, University of Glasgow, Glasgow G12 8QQ, UK
[2] Scottish Centre for Nanotechnology in Construction Materials, School of Engineering Sciences, University of Paisley, Paisley PA1 2BE, UK

[*Received 25 October 2007; Accepted 15 April 2008*]

ABSTRACT

Calcium carbonate biominerals are frequently analysed in materials science due to their abundance, diversity and unique material properties. Aragonite nacre is intensively studied, but less information is available about the material properties of biogenic calcite, despite its occurrence in a wide range of structures in different organisms. In particular, there is insufficient knowledge about how preferential crystallographic orientations influence these material properties. Here, we study the influence of crystallography on material properties in calcite semi-nacre and fibres of brachiopod shells using nano-indentation and electron backscatter diffraction (EBSD). The nano-indentation results show that calcite semi-nacre is a harder and stiffer (H $\approx$ 3–5 GPa; E = 50–85 GPa) biomineral structure than calcite fibres (H = 0.4–3 GPa; E = 30–60 GPa). The integration of EBSD to these studies has revealed a relationship between the crystallography and material properties at high spatial resolution for calcite semi-nacre. The presence of crystals with the *c*-axis perpendicular to the plane-of-view in longitudinal section increases hardness and stiffness. The present study determines how nano-indentation and EBSD can be combined to provide a detailed understanding of biomineral structures and their analysis for application in materials science.

KEYWORDS: biomineral, nano-indentation, electron backscatter diffraction (EBSD), *c* axis, calcite, brachiopods.

Introduction

MINERAL-PRODUCING organisms exert exquisite control on all aspects of biomineral production including the development of a wide range of structures using the same basic chemical components. Calcium carbonate biomineral structures, due to their abundance, diversity and unique material properties, are frequently analysed in materials science (Lowenstam and Weiner, 1989; Heuer *et al.*, 1992). Aragonite nacre is intensively studied because of its excellent mechanical properties (Feng *et al.*, 2000; Hou and Feng, 2003; Katti *et al.*, 2005) and the possibility of mimicking its structure at the nanoscale (Katti *et al.*, 2005). Less information, however, is available about material properties of biogenic calcite, despite its occurrence in a wide range of structures in different organisms. In addition to structural investigations, an understanding of the relationship between material properties and crystallography is required. Preferential crystallographic orientations enhance the material properties of aragonite nacre (Bruet *et al.*, 2005; Kearney *et al.*, 2006) and calcite fibres (Schmahl *et al.*, 2004; Pérez-Huerta *et al.*, 2007). However, an assessment of the relationship between material properties and crystallography of calcite in the context of shell ultrastructure is not currently available at high spatial resolution.

Here, we use a combination of nano-indentation and electron backscatter diffraction (EBSD) to conduct a detailed assessment of the material

* E-mail: maggie.cusack@ges.gla.ac.uk
DOI: 10.1180/minmag.2008.072.2.563

properties and crystallography of two calcite brachiopods with different shell ultrastructures. The craniid brachiopod, *Novocrania anomala*, has a shell composed of calcite semi-nacre, similar in morphology to nacre but with more frequent screw dislocations (England *et al.*, 2007), while the rhynchonelliform brachiopod, *Terebratulina retusa*, is composed of calcite fibres. Values of hardness (H) and the Young's modulus of elasticity (E) were already evaluated by nano-indentation to determine the material properties of calcite semi-nacre and fibres (Pérez-Huerta *et al.*, 2007; see summary in Tables 1 and 2). Electron backscatter diffraction (EBSD) is used to determine crystallographic variation for each shell ultrastructure in reference to the *c* axis of calcite crystals. The combination of both techniques is focused on the analysis of the secondary layer of both brachiopod species, which comprises the majority of the shell thickness. Finally, results from both techniques are integrated to assess a possible relationship between material properties and crystallography.

Material and methods

Material

Two recent species of calcite brachiopods, *Terebratulina retusa* and *Novocrania anomala*, were used for this study. The biological information of these organisms is given by Pérez-Huerta *et al.* (2007). Articulated mature specimens of both brachiopods were collected at 200 m water depth from the same locality in the Firth of Lorn (Oban), NW of Scotland. Valves were disarticulated and the pedicle and soft tissues removed using dental tools. Valves were then cleaned in an ultrasonic bath using an aqueous solution of sodium hypochlorite (1% v/v) and thoroughly rinsed in MilliQ^{TM} water. Finally, valves were dried at ambient temperature to avoid the influence of differences in hydration on mechanical properties. 2D sections of shell samples were obtained from posterior-anterior cuts along the plane of symmetry of the dorsal valves (Pérez-Huerta *et al.*, 2007).

Nano-indentation

Previous measurements of material properties of biominerals (e.g. Lichtenegger *et al.*, 2002), including brachiopods (Pérez-Huerta *et al.*, 2007; Griesshaber *et al*., 2007), have used nano-indentation. Measurements were performed in three regions (posterior, central and anterior) along the dorsal valve length of *Novocrania anomala* (Na) and *Terebratulina retusa* (Tr) (Pérez-Huerta *et al.*, 2007). Nano-indentations have to be performed on highly-polished surfaces to avoid variations in measurements due to topographical effects (e.g. roughness). The 2D sections of dorsal valves were partially embedded in araldite resin leaving the top surface free of any resin. Subsequently, the surface was ultra-polished initially with 6 and 3 μm diamond paste and finally polished using Al oxide (1 and 0.3 μm) and then colloidal silica (0.6 μm).

Methods have already been established for the determination of micro-mechanical properties of a material using depth-sensing indentation. The methodology and operating principle for the nano-indentation technique are reviewed and presented in detail elsewhere (Oliver and Pharr, 1992, 2004). A typical outcome of the micro/nano-indentation testing is an indentation load-depth hysteresis curve. As a load is applied to an indenter in contact with a specimen surface, an indent/impression is produced which consists of permanent/plastic deformation and temporary/elastic deformation. Recovery of the elastic deformation occurs when unloading is started. Determination of the elastic recovery by analysing the initial part of the unloading data according to a model for the elastic contact problem leads to a solution for calculation of the elastic modulus (E) and hardness (H) of the test area.

A Nanoindenter XP from MTS Systems Corporation was used. All testing was programmed in such a way that the loading started when the indenter came into contact with the test surface and the load maintained for 30 s at the pre-specified maximum value before unloading. Progressive multi-step indentation testing with 3–5 loading-unloading cycles at different depths was applied at each test point. The unloading data for the lower indentation depth (h_p = ~100 nm for Na and h_p = ~1000 nm for Tr, respectively) was used to determine the modulus and hardness values of the indentation point, whereas the indent produced at the greater depth (h_p = ~2000 nm) allows easy examination of the indent and the tested area using optical and scanning electron microscopes (SEM). The selection of different loads (thus the different indentation-depth levels mentioned above) for studying the two types of sample (Na and Tr) aimed at measuring the mechanical properties of

the basic structural elements for the two specimens which are calcite fibres of ~20 μm diameter in Tr and calcite tablets of 0.5−1 μm thickness in Na. An indentation grid across the shell layers varying from 2×15 to 4×10 indents (depending on the thickness of the layers at the selected test location on the specimen) was applied with an indent spacing of 20 μm so as to avoid overlapping of the indents.

The load-displacement curves together with optical microscopic images of the indents were examined in order to verify the validity of each indentation measurement. A small proportion (5−10%) of the load-displacement curves showed a sudden increase in displacement with little increase in load, which is usually associated with cracks, local/surface defects and interfaces of different layers. The curves were easily detected and excluded from the analysis. Another type of irregular load-displacement curve, which shows a much greater creep (e.g. increase of displacement with time during the load-holding segment) and reduced stiffness, was also detected on a few spots of mainly organic matter and thus, also excluded from the final analysis.

Electron backscatter diffraction

Polished shell sections were coated with a thin layer of carbon and surrounded by silver paint to avoid electron charging. Areas adjacent to where the nano-indentation experiments were performed were analysed in an FEI 200F field-emission environmental SEM in high vacuum mode with an aperture and spot size of 4. The stage was tilted 70º and the electron beam diffracted by interaction of crystal planes in the shell sample. The diffracted beam interacts with a phosphor screen producing a series of Kikuchi bands that enable crystal identification and orientation to be determined. Data is filtered to remove all data points below a confidence index (CI) of 0.1 and the filtered data analysed using (free OIM version) software from EDAX.

Results

Hardness (H) and elastic modulus (E) were mapped throughout the thickness of the secondary layer of *Novocrania anomala* and *Terebratulina retusa* in three regions along the dorsal valve length (Pérez-Huerta *et al.*, 2007) (Tables 1 and 2). The assessment of crystallographic influence on these material properties is based on the combination of results by nano-indentation and electron backscatter diffraction (EBSD).

In *Novocrania anomala*, values of hardness and elastic modulus in the secondary layer are very uniform within each region of the valve, with the central and anterior regions harder and stiffer than the posterior area (Fig. 1) (Table 1). This is mainly explained by the presence of continuous and thick bands progressing from the outside to the inside where hardness and stiffness increase by an order of magnitude (Fig. 1). The ultrastructure provides no explanation for this observation. The crystallography, however, indicates that these bands are dominated by calcite crystals with the *c* axis normal to the plane of view (Fig. 1). This crystallographic orientation correlates with an increase in stiffness and hardness not only in the central region but also in localized areas of the posterior and anterior regions (Fig. 1). In addition, the posterior region

TABLE 1. Summary of nano-indentation results of elastic modulus (E) and hardness (H) for *N. anomala* (Na) (~100 nm depth) and *T. retusa* (Tr) (~2000 nm depth).

Na	Mechanical properties of materials (mean value ± standard deviation)					
	a: posterior		b: central		c: anterior	
	E (GPa)	H (GPa)	E (GPa)	H (GPa)	E (GPa)	H (GPa)
Sl	59.81±10.79	2.68±0.94	69.24±16.52	3.88±1.24	71.82±9.31	3.89±0.58
Tr						
So	30.82±4.03	0.88±0.26	53.21±5.34	1.92±0.22	55.71±5.43	2.10±0.24
Si	37.33±2.41	1.07±0.13	28.03±4.36	0.88±0.21	50.50±6.42	1.55±0.40
Sim	27.76±n.a.*	0.79±n.a.*	34.03±5.33	0.99±0.35	32.83±5.68	0.83±0.12

* Only single result available

Sl: secondary layer; So: outer secondary layer; Si: inner secondary layer; Sim: innermost secondary layer.

TABLE 2. Summary of ANOVA for comparison of elastic modulus (E) and hardness (H) for *N. anomala* (Na) and *T. retusa* (Tr).

Groups	Count	Sum	Average	Variance
Na (E)	131	8924.282	68.12429	198.0709
Tr (E)	52	2103.788	40.45747	118.367

ANOVA (Single Factor) Source of variation	SS	df	MS	F	P-value	F crit.
Between groups	28493.25	1	28493.25	162.2504	6.02×10^{-27}	3.893349
Within groups	31785.93	181	175.6129			
Total	60279.19	182				

Groups	Count	Sum	Average	Variance
Tr (H)	52	67.25823	1.293427	0.260612
Na (H)	131	476.2635	3.635599	1.24471

ANOVA (Single Factor) Source of variation	SS	df	MS	F	P-value	F crit.
Between groups	204.2025	1	204.2025	211.0789	3.35×10^{-32}	3.893349
Within groups	175.1035	181	0.967422			
Total	379.3059	182				

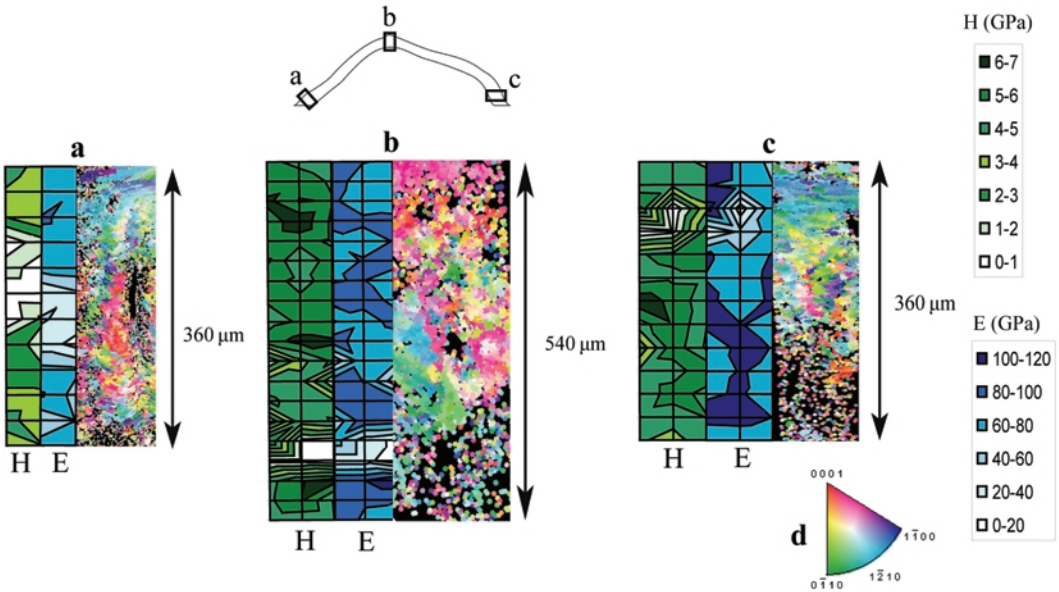

FIG. 1. Maps of nano-indentation values of hardness (H) and elastic modulus (E) and electron backscatter diffraction (EBSD) (spatial resolution: 1 µm), showing: (*a*) crystallographic orientation of calcite crystals (*d*: crystallographic key indicating colour coding of crystallographic planes) in the secondary layer of the posterior (2 × 20 indents, 20 µm across); (*b*) central (3 × 20 indents, 60 µm across); and (*c*) anterior (3 × 20 indents, 60 µm across) regions of the dorsal valve of *Novocrania anomala*.

is softer and less stiff than the central and anterior regions, possibly as a consequence of a larger concentration of organic components in this region. Finally, the values of hardness and elastic modulus (H ≈ 2−5 GPa and E ≈ 50−80 GPa) of *Novocrania anomala* are close to those determined for inorganic calcite (H >3 GPa and E >85 GPa) (Züegner *et al.*, 2006).

In *Terebratulina retusa*, variations in material properties clearly correlate with structural differentiation while the crystallographic orientation, with the *c* axis perpendicular to the shell surface is constant in the studied areas (Fig. 2). An exception to this trend is observed in the posterior region where hardness and stiffness are quite uniform across the valve thickness. This posterior region is softer and less stiff than the other regions along the valve, which may be a result of a large concentration of organic material. In contrast, the anterior and central regions reflect a relationship between structure and material properties. The outer part of the secondary layer (So) is harder and stiffer than the inner part (Si) (Table 1) (Fig. 2), although both layers contain calcite fibres. The inner part of the secondary layer (Si) is very distinct with smaller values of hardness (0.6−2 GPa) and elastic modulus (24−56 GPa). This difference within the secondary layer is likely to be because the inner part is composed of more compactly emplaced calcite fibres. The higher degree of compaction, which provides a better surface to distribute stress, is caused by a large amount of organic matrix bounding the fibres. The organic content and compaction result in a softer and less-stiff inner part of the secondary layer.

Discussion

Detailed studies of material properties at this high spatial resolution provide a basis for general comparison between brachiopod species (Tables 1 and 2). Although the nano-indentation studies were performed on 2D sections obtained from posterior-anterior cuts along the plane of symmetry, it is possible to generalize the results for the whole dorsal valve based on studies of synthetic crystals (Schall *et al.*, 2006). Thus, *Novocrania anomala* is harder and stiffer (H ≈ 3−5 GPa; E ≈ 50−85 GPa) than *Terebratulina retusa* (H = 0.4−3 GPa; E = 30−60 GPa) (Tables 1 and 2). These material properties are a consequence of the ultrastructure of the secondary layer since it comprises the majority of the shell thickness (Pérez-Huerta *et al.*, 2007). Calcite semi-nacre, therefore, provides a harder and stiffer shell structure than calcite fibres. Although the type of structure is the main factor controlling the material properties in these calcite shells, variations in crystallography influence these properties. In calcite semi-nacre, the presence of crystals with the *c* axis perpendicular to the plane of view in longitudinal section increase hardness and stiffness (Fig. 1; Table 1). The constancy of the crystallographic orientation of the calcite fibres in the areas studied in *T. retusa* shells, precludes any observations on correlations between crystallographic orientation and material properties

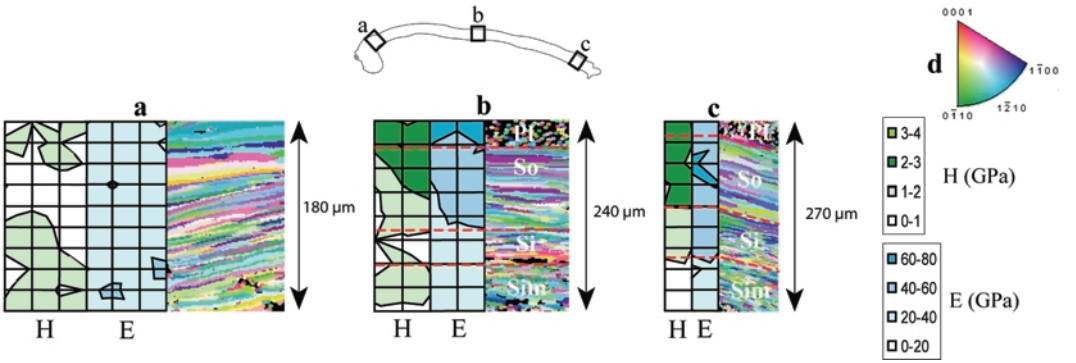

FIG. 2. Maps of nano-indentation values of hardness (H) and elastic modulus (E) and electron backscatter diffraction (EBSD) (spatial resolution: 2 µm), showing crystallographic orientation of calcite crystals (*d*: crystallographic key indicating colour coding of crystallographic planes) in (*a*) the posterior (4 × 15 indents, 60 µm across); (*b*) central (3 × 15 indents, 60 µm across); and (*c*) anterior (2 × 15 indents, 30 µm across) regions of the dorsal valve of *Terebatulina retusa* (Pl: primary layer; So: outer secondary layer; Si: inner secondary layer; Sim: innermost secondary layer).

(Fig. 2). In addition to structure and crystallography, the organic content seems to be an important factor determining material properties. The posterior region of both brachiopod species contains a large amount of organic material that correlates with a significant drop in hardness and stiffness.

Conclusions

We have used nano-indentation to determine the material properties of two types of biogenic calcite. The integration of EBSD to these studies has also established a relationship between the crystallography and material properties at high spatial resolution. This study has demonstrated how both techniques can be combined to provide a detailed understanding of biomineral structures in their application for materials science.

Acknowledgements

A. Pérez-Huerta and M. Cusack thank the BBSRC (BB/E003265/1) for funding and A. Pérez-Huerta thanks the Mineralogical Society (UK) for a Senior Travel Bursary Award. We also thank J. Gilleece, P. Chung, R. McDonald, L. Hill and Y. Finlayson for technical support. An earlier version of this manuscript benefited from comments by two colleagues.

References

Bruet, B.J.F., Qi, H.J., Boyce, M.C., Panas, R., Tai, K., Frick, L. and Ortiz, C. (2005) Nanoscale morphology and indentation of individual nacre tablets from the gastropod mollusc *Trochus niloticus*. *Journal of Materials Research*, **20**, 2400–2419.

England, J., Cusack, M., Dalbeck, P. and Pérez-Huerta, A. (2007) Comparison of the crystallographic structure of semi nacre and nacre by electron backscatter diffraction. *Crystal Growth and Design*, **7**, 307–310.

Feng, Q.L., Cui, F.Z., Pu, G., Wang, R.Z. and Li, H.D. (2000) Crystal orientation, toughening mechanisms and a mimic of nacre. *Materials Science Engineering C*, **11**, 19–25.

Griesshaber, E., Schmahl, W.W., Neuser, R., Pettke, T., Blüm, M., Mutterlose, J. and Brand, U. (2007) Crystallographic texture and microstructure of terebratulide brachiopod shell calcite: An optimized materials design with hierarchical architecture. *American Mineralogist*, **92**, 722–734.

Heuer, A.H., Fink, D.J., Laraia, V.J., Arias, J.L., Calvert, P.D., Kendall, K., Messing, G.L., Blackwell, J., Rieke, P.C., Thompson, D.H., Wheeler, A.P., Veis, A. and Caplan, A.I. (1992) Innovative materials processing strategies – A biomimetic approach. *Science*, **255**, 1098–1105.

Hou, W.T. and Feng, Q.L. (2003) Crystal orientation preference and formation mechanism of nacreous layer in mussel. *Journal of Crystal Growth*, **258**, 402–408.

Katti, K., Katti, D.R., Tang, J., Pradhan, S. and Sarikaya, M. (2005) Modeling mechanical responses in a laminated biocomposite. Part II. Nonlinear responses and nuances of nanostructure. *Journal of Materials Science*, **40**, 1749–1755.

Kearney, C., Zhao, Z., Bruet, B.J.F., Radovitzky, R., Boyce, M.C. and Ortiz, C. (2006) Nanoscale anisotropic plastic deformation in single crystal aragonite. *Physical Review Letters*, **96**, 255505.

Lichtenegger, H.C., Schöberl, T., Bartl, M.H., Waite, H. and Stucky, G.D. (2002) High abrasion resistance with sparse mineralization: Copper biomineralization in worm jaws. *Science*, **298**, 389–392.

Lowenstam, H.A. and Weiner, S. (1989) *On Biomineralization*. Oxford University Press, New York, 324 pp.

Oliver, W.C. and Pharr, G.M. (1992) An improved technique for determining hardness and elastic modulus using load and displacement sensing indentation experiments. *Journal of Materials Research*, **7**, 1564–1579.

Oliver, W.C. and Pharr, G.M. (2004) Measurements of hardness and elastic modulus by instrumented indentation: Advances in understanding and refinements to methodology. *Journal of Materials Research*, **19**, 3–20.

Pérez-Huerta, A., Cusack, M., Zhu, W., England, J. and Hughes, J. (2007) Material properties of brachiopod shell ultrastructure by nanoindentation. *Journal of the Royal Society Interface*, **4**, 33–39.

Schall, P., Cohen, I., Weitz, D.A. and Spaepen, F. (2006) Visualizing dislocation nucleation by indenting colloidal crystals. *Nature*, **440**, 319–323.

Schmahl, W.W., Griesshaber, E., Neuser, R., Lenze, A., Job, R. and Brand, U. (2004) The microstructure of the fibrous layer of terebratulide brachiopod shell calcite. *European Journal of Mineralogy*, **16**, 693–697.

Züegner, S., Marquardt, K. and Zimmermann, I. (2006) Influence of nanomechanical crystal properties on the comminution process of particulate solids in spiral jet mills. *European Journal of Pharmaceutics and Biopharmaceutics*, **62**, 194–201.